



PAPER

FRESH 3D bioprinting a contractile heart tube using human stem cell-derived cardiomyocytes

To cite this article: Jacqueline Bliley *et al* 2022 *Biofabrication* 14 024106

View the [article online](#) for updates and enhancements.

You may also like

- [A biofabrication method to align cells within bioprinted photocrosslinkable and cell-degradable hydrogel constructs via embedded fibers](#)
Margaret E Prendergast, Matthew D Davidson and Jason A Burdick
- [4D bioprintable self-healing hydrogel with shape memory and cryopreserving properties](#)
Shin-Da Wu and Shan-hui Hsu
- [The emergence of 3D bioprinting in organ-on-chip systems](#)
Kirsten Fetah, Peyton Tebon, Marcus J Goudie *et al.*



Breath Biopsy[®] OMNI

The most advanced, complete solution for global breath biomarker analysis

SEE WHAT OMNI
CAN DO FOR YOU



Expert Study Design
& Management



Robust Breath
Collection



Reliable Sample
Processing & Analysis



In-depth Data
Analysis



Specialist Data
Interpretation

Biofabrication



PAPER

FRESH 3D bioprinting a contractile heart tube using human stem cell-derived cardiomyocytes

RECEIVED
5 December 2021

ACCEPTED FOR PUBLICATION
25 February 2022

PUBLISHED
16 March 2022

Jacqueline Bliley¹ , Joshua Tashman¹ , Maria Stang² , Brian Coffin² , Daniel Shiwarski¹ , Andrew Lee¹ , Thomas Hinton¹  and Adam Feinberg^{1,2,*} 

¹ Department of Biomedical Engineering, Carnegie Mellon University, Pittsburgh, PA, United States of America

² Department of Materials Science & Engineering, Carnegie Mellon University, Pittsburgh, PA, United States of America

* Author to whom any correspondence should be addressed.

E-mail: feinberg@andrew.cmu.edu

Keywords: heart tube, bioprinting, engineered heart tissue, heart muscle, FRESH

Supplementary material for this article is available [online](#)

Abstract

Here we report the 3D bioprinting of a simplified model of the heart, similar to that observed in embryonic development, where the heart is a linear tube that pumps blood and nutrients to the growing embryo. To this end, we engineered a bioinspired model of the human heart tube using freeform reversible of embedding of suspended hydrogels 3D bioprinting. The 3D bioprinted heart tubes were cellularized using human stem cell-derived cardiomyocytes and cardiac fibroblasts and formed patent, perfusable constructs. Synchronous contractions were achieved $\sim 3\text{--}4$ days after fabrication and were maintained for up to a month. Immunofluorescent staining confirmed large, interconnected networks of sarcomeric alpha actinin-positive cardiomyocytes. Electrophysiology was assessed using calcium imaging and demonstrated anisotropic calcium wave propagation along the heart tube with a conduction velocity of $\sim 5\text{ cm s}^{-1}$. Contractility and function was demonstrated by tracking the movement of fluorescent beads within the lumen to estimate fluid displacement and bead velocity. These results establish the feasibility of creating a 3D bioprinted human heart tube and serve as an initial step towards engineering more complex heart muscle structures.

1. Introduction

Heart failure affects more than 26 million people worldwide and more than half of those patients will die within five years of diagnosis [1, 2]. While there are many underlying causes, current pharmaceutical treatments and medical devices can only slow disease progression. The only long-term solution for end-stage heart failure is transplantation [3], but donor organs are in limited supply and address only a small fraction of patients in need [4]. A key challenge is that the adult human heart has minimal regenerative capacity and cannot repair the damage due to myocardial infarction (MI) and other diseases [5]. Human embryonic stem cells (ESCs) and induced-pluripotent stem cells can be differentiated into new cardiomyocytes providing a potential path to regeneration [6]. Indeed, recent work injecting stem cell-derived cardiomyocytes into the mammalian heart

post-MI has shown the ability to achieve remuscularization [7, 8]. However, generating sufficient quantities and engineering these stem cell-derived cardiomyocytes into functional cardiac muscle remains an ongoing challenge in the field [9].

Here we sought to engineer a contractile model of the human heart as early proof-of-concept of organ-scale biofabrication using stem cell-derived cardiomyocytes. Since the adult four-chambered heart is highly complex, as an alternative approach we focused on building a simpler heart structure, like that observed during embryonic development. Specifically, during early cardiogenesis the heart exists as a linear tube that then bends, loops, and septates to form the mature four-chambered structure [10]. The linear heart tube, while structurally much simpler, still displays hallmarks of cardiac function including action potential propagation, synchronized contraction, and the ability to pump fluid. To build the linear

heart tube we used freeform reversible embedding of suspended hydrogels (FRESH) 3D bioprinting [11], which allows for the printing of soft materials including biopolymers, like collagen, into cellularized cardiac tissue [12]. Our objective was to create a bioinspired model of the embryonic heart tube and assess its structure and functional outputs, including electrophysiology and contractility.

2. Materials and methods

2.1. Cardiomyocyte differentiation/purification

Cardiomyocytes were differentiated from HES3 (ES03, Wicell) ESCs using mesoderm induction and cardiac specification according to previously described methods [13, 14]. The HES3 ESCs were maintained in Essential 8 (E8) medium (A1517001, Life Technologies) on $12 \mu\text{g cm}^{-2}$, Geltrex (A1413301, Life Technologies)-coated six well plates and passaged every four days ($\sim 80\%$ confluence). To prepare for differentiation, HES3 ESCs were seeded at $8000 \text{ cells cm}^{-2}$ in Geltrex coated T75 flasks with daily E8 media changes for three days. At 80% confluence (day 0 of differentiation), cells were washed with $1\times$ phosphate buffered saline (PBS) and media was switched to RPMI 1640 (21870076, Thermofisher) supplemented with 1% v/v L-glutamine (25030081, Thermofisher), B27 supplement (17504044, Thermofisher), and $6 \mu\text{M}$ CHIR99201 (C-6556, LC laboratories). On day 2 of differentiation, cells were washed with $1\times$ PBS and media was changed to RPMI 1640 supplemented with 1% v/v L-glutamine, B27 supplement, and $2 \mu\text{M}$ Wnt C-59 (S7037, Selleck Chemicals). On days 4 and 6, cells were switched to RPMI 1640 media containing 1% v/v L-glutamine and B27 supplement. On days 8 and 10, medium was changed to CDM3 media, consisting of RPMI 1640 supplemented with 1% v/v L glutamine, $213 \mu\text{g ml}^{-1}$ L-Ascorbic acid 2-phosphate sesquimagnesium salt hydrate $>95\%$ (A8960, Sigma), and $500 \mu\text{g ml}^{-1}$ human albumin (A9731, Sigma). On day 12, spontaneously beating cells were passaged for lactate-based metabolic selection of cardiomyocytes [15].

To passage for cardiomyocyte purification, cells were incubated with TrypLE for 15 min at 37°C to enable single cell dissociation. Cells were then reseeded in CDM3L, consisting of RPMI 1640 without glucose (11879020, Thermofisher) supplemented with 7.1 mM sodium-lactate (L4263, Sigma), $213 \mu\text{g ml}^{-1}$ L-Ascorbic acid 2-phosphate sesquimagnesium salt hydrate $>95\%$, and $500 \mu\text{g ml}^{-1}$ human albumin. Cells were maintained in CDM3L for several days before replacing back to CDM3 medium.

2.2. Fibroblast culture

Normal human primary ventricular cardiac fibroblasts (CC-2904, Lonza) were obtained and cultured via manufacturer's instructions. Fibroblasts

were cultured at an initial density of $5000 \text{ cells cm}^{-2}$ in FGM-3 media (CC-4526, Lonza) and passaged prior to reaching 80% confluence. Fibroblasts were used between passage 5 and passage 8 for these studies.

2.3. Bioprinter setup

A custom high-precision bioprinter was assembled using a precision ballscrew z stage (MX80S, Parker-Hannefin) and a microscope stage (H117, Prior Scientific) mounted in a cartesian setup using extruded aluminum profiles. Mounted to the Z stage was a Replistruder 4 high-precision open-source syringe pump [16], used with a 2.5 ml gastight syringe (1000 series, Hamilton). The stages and syringe pump were controlled using a Duet 3 6HC (Duet3D) motion control board with a Raspberry Pi microcontroller running a dedicated user interface with mouse, keyboard, and display.

2.4. FRESH slurry support bath generation

FRESH v2.0 gelatin support bath was prepared using previously described methods [12]. Briefly, 2% w/v Gelatin B (G7, Fisher Chemicals), 0.25% w/v Pluronic® F-127 (P2443, Sigma Aldrich), and 0.5% w/v Gum Arabic (G9752, Sigma-Aldrich) were dissolved in 50% v/v ethanol solution at 45°C in a 1 l beaker. The pH was then adjusted to 5.8 by dropwise addition of 2 M hydrochloric acid. The beaker was then placed under an overhead stirrer at $\sim 600 \text{ RPM}$ (IKA, Model RW20), sealed with parafilm, and allowed to cool to room temperature while stirring overnight. The resulting slurry was evenly distributed in 50 ml conical tubes and centrifuged at 300 g for 3 min. The slurry was then washed three times in distilled water followed by three times in 50 mM HEPES (61-034-RO, Corning) with centrifuging at 2000 g for 3 min. The washed slurry was stored at 4°C prior to printing.

2.5. FRESH printing of heart tubes

Digital models of the heart tube were created using Fusion 360 (Autodesk) computer aided design (CAD) software and then exported as a Standard Tessellation Language (STL) file format. To generate G-code instructions for the printer, STL files were sliced in Slic3r (version 1.3.0, <https://slic3r.org/>). In general, slicer settings were a print speed of 10 mm s^{-1} , 2 perimeters, 30% infill, $35 \mu\text{m}$ layer height, 0.15 mm retraction length, and a 1 mm z-hop. Collagen type I bioink (LifeInk 200, Advanced Biomatrix) was prepared by addition of 0.24 M acetic acid in a 2:1 ratio with the 35 mg ml^{-1} collagen stock concentration to create a 24 mg ml^{-1} acidic collagen solution. This bioink was then centrifuged at 3000 g for 5 min to remove air bubbles and transferred to a gas-tight, 2.5 ml syringe with a 34 gauge needle (JG34-0.25HPX, Jensen Global). To compact the support bath for printing, tubes were degassed for 30 min

to remove air bubbles and then centrifuged at 1800 g for 3 min. The supernatant was removed, and compacted slurry was transferred to a Petri dish and secured onto the print bed. Upon print completion, the Petri dish was removed from the print bed and placed in a 37 °C incubator for 45 min to melt the support bath. Prints were then transferred to 50 mM HEPES solution and placed in a rotating 37 °C incubator for 1 h to remove excess gelatin. Finally, printed heart tubes were sterilized with UV for 15 min and stored in 50 mM HEPES supplemented with 1% v/v penicillin streptomycin prior to cardiomyocyte casting.

2.6. Optical imaging of printed heart tubes

Printed heart tubes were imaged under brightfield with a stereomicroscope (SMZ1000, Nikon) using both a digital SLR camera (Model 70D, Canon) and a Prime 95B Scientific CMOS camera (Photometrics). In addition, 3D imaging was performed using a 1300 nm optical coherence tomography (OCT) system (VEG210C1, ThorLabs). ImageJ and Imaris 9.1 (Bitplane) were used for visualization and 3D renderings. For OCT imaging both 2D linescan and 3D volumetric imaging modes were used.

2.7. Heart muscle tissue casting and culture

To hold the printed heart tubes in place during the tissue casting process, polydimethylsiloxane (PDMS) wells were first created. To do this, negative molds were 3D printed with acrylonitrile butadiene styrene (ABS) plastic (MK3S+, Prusa) and then PDMS was cast around them in six well plates and cured overnight at 65 °C. The Sylgard 184 PDMS (Dow Corning) was mixed at a 10:1 weight ratio of base to curing agent in a Thinky conditioning mixer (Phoenix Equipment Inc.) using a 2 min 2000 RPM mixing cycle followed by a 2 min 2000 RPM defoaming cycle. The PDMS wells in the 6 well plate were then sterilized with UV-Ozone for 15 min. PDMS wells were treated with 1% w/v Pluronic® F-127 to limit casted tissue attachment to the PDMS well. Sterile heart tubes were then placed in the PDMS wells and submerged in sterile 50 mM HEPES with 1% v/v penicillin-streptomycin until tissue casting.

To cast cardiac tissue around the printed tubes, cardiomyocytes and fibroblasts were combined in a 9:1 ratio within a mixture of collagen type I derived from rat tail (354249, Corning) and Matrigel (354263, Corning) at a final concentration of 30 million cells ml⁻¹. The final concentrations were 1 mg ml⁻¹ collagen type I, 1.7 mg ml⁻¹ Matrigel, 10% 10X PBS, and 2.3% 1 N NaOH. Next, the HEPES solution was removed from the PDMS wells and each printed tube was covered with 275 µl of cell and extracellular matrix (ECM) solution. Constructs were then incubated at 37 °C for 1 h to gel collagen and Matrigel and then covered in media consisting of RPMI 1640 supplemented with 1% v/v KnockOut™ Serum

Replacement (10828028, Thermofisher) and 1:1000 MycoZap Plus CL (VZA-2012, Lonza). Heart tubes were maintained in media for 14 days, which was changed every 2 days.

2.8. Contractility analysis

To determine if heart tubes were capable of pumping fluid, fluorescent beads (556286, BD Biosciences) were slowly injected into the tube lumen and were allowed to settle for 5 min following injection. This was done to ensure that movement of the beads was not due to fluid movement associated with the injection process. Tubes were imaged on a custom heated stage using a fluorescent stereomicroscope (SMZ1000, Nikon) equipped with DAPI, GFP, and TRITC filters, an X-Cite lamp (Excelitas), and a Prime 95B Scientific CMOS camera. Videos of the bead displacement at the tube lumen following spontaneous and electrically stimulated cyclical contractions of the heart tube were recorded up to 100 frames per second. To track the beads, the IMARIS 9.1 spot tracking algorithm was used. Peak and average bead velocity were calculated. Peak bead velocity was defined as the maximum displacement of the bead during contraction divided by the time it took for this displacement to occur whereas average bead velocity was defined as the average displacement over three contractions divided by the time.

2.9. Electrical stimulation and calcium imaging

Calcium imaging was performed on heart tubes during spontaneous and paced contractions after 14 days in culture. Briefly, heart tubes were stained with Cal520 (21130, AAT Bioquest) based on previously described methods [12]. An excitation-contraction decoupler, 10 µM Blebbistatin (B0560, Sigma), was used to prevent spontaneous contractions of the heart tubes that would preclude automated analysis. Heart tubes were field stimulated using paired parallel platinum electrodes immersed in the Tyrodes solution and point stimulated with a concentric bipolar microelectrode (30202, FHC Inc.) composed of an inner platinum-iridium pole and outer stainless-steel pole. Tubes were imaged on a custom heated stage maintaining the temperature at 37 ± 1 °C using the fluorescent stereomicroscope. Calcium transients were analyzed using custom MATLAB code (R2019, MathWorks) using signal peak times and cross correlation to create activations maps and calculate conduction velocities, as previously published [12].

2.10. Immunofluorescent imaging and analysis

Heart tubes were stained and imaged whole mount to assess the structure. Tubes were fixed in 4% paraformaldehyde (Electron Microscope Sciences) in 1X PBS supplemented with 1:200 Triton-X 100 (9002-93-1, Sigma) for 1 h. Next, tubes were washed 3 times for 30 min each in 1X PBS on a rotary shaker. Samples were then blocked in 5% goat serum in 1× PBS

overnight on a shaker followed by washing 3 times for 30 min in 1X PBS. Mouse anti-sarcomeric α -actinin antibody (A7811, Sigma-Aldrich) was diluted to 1:100 in 1X PBS and incubated with the tissues overnight on a shaker. Tubes were then washed 3 times for 30 min each in 1X PBS before incubating with 1:200 DAPI (D1306, Molecular Probes), 3:200 phalloidin conjugated with Alexa-Fluor 488 (A12379, Life Technologies), and 1:100 goat anti-mouse antibody conjugated with Alexa-Fluor 555 (A21422, Life Technologies) in PBS overnight on a shaker. After the final incubation step, samples were rinsed 3 times for 30 min each in 1X PBS. The fluorescently stained heart tubes were imaged with two different confocal microscopes (A1R, Nikon and LSM 700, Zeiss).

2.11. Statistics

All graphs were created and statistical analyses performed using GraphPad Prism 7. Data are presented as mean \pm standard deviation and assessed for normality using Shapiro–Wilk normality test and homogeneity of variances with Brown–Forsythe test. T-tests were used to compare data with two groups. Welch’s correction was used on data that had unequal standard deviations. To compare multiple groups, Kruskal–Wallis test was performed. If statistical significance was found, Dunn’s multiple comparison test was used to evaluate differences between each group.

3. Results

3.1. Heart tube printing

To create the collagen heart tube, we used CAD to design a linear tube with supports on either end (figure 1(a)). The tube had a 1.4 mm inner diameter, 2.0 mm outer diameter, and 300 μm wall thickness. While these dimensions are larger than the embryonic heart tube, which has an inner diameter of $\sim 300 \mu\text{m}$ [10], our goal was to test basic feasibility at a length scale our bioprinter could reliably fabricate. The model of the tube was processed into g-code for 3D printing, and the collagen extrusions for the tube wall were oriented along the longitudinal axis (figure 1(b)). Heart tubes were FRESH 3D bioprinted using acidified type I collagen bioink (24 mg ml⁻¹) using established methods (figure 1(c)), where the printed collagen rapidly gels due to pH-driven neutralization by the buffered gelatin support bath [12]. Following printing, melting of the support bath at 37 °C further gels the collagen and then releases the printed structure. To verify print fidelity, we used a combination of brightfield imaging and optical coherence tomography (OCT). Results demonstrate that the tubes were printed with high fidelity and with no visible defects (figures 1(d) and (e)). It is notable that there was no stringing (unwanted extrusion of printed material out of the needle as it travels to a different place) or crowning

(over-extrusion of material). Further, OCT of the printed tube confirmed that tube lumens were patent and displayed consistent wall thickness of $\sim 300 \mu\text{m}$, demonstrating that we were able to print the tube design with high fidelity (figures 1(f) and (g)).

3.2. Formation of cellularized heart tubes

To create the cellularized heart tubes in this study, collagen tubes were placed in custom-fabricated PDMS wells (figure 2(a)) designed to create a well around the tube for cell seeding. Rather than 3D printing the cardiac cells directly, we used a casting approach in order to rapidly cellularize many scaffolds and minimize cell handling time. Similar to other previous engineered heart muscle tissue studies, we cast collagen gels containing a 9:1 ratio of cardiomyocytes to cardiac fibroblasts [17–20] around the 3D printed collagen tube (figure 2(b)), where this has been shown to improve the formation of contractile cardiac tissues through cardiac fibroblast-drive ECM remodeling and promotion of cardiomyocyte organization. Comparable to cast cardiac tissues in the literature [17, 21], the cells rapidly compacted the gel around the collagen tubes to form a dense tissue layer (figure 2(c)). It is important to note that we performed several iterations on our initial tube design to confirm we were getting consistent heart tube formation. Our first design consisted of a tube suspended over a 3D printed collagen well (supplemental figures 1(a) and (b) available online at stacks.iop.org/BF/14/024106/mmedia). With this design (supplemental figure 1(c)), we would sometimes observe tissue attachment to the collagen well resulting in failed tube formation (supplemental figure 1(d)). Since removing this collagen well, we have observed consistent and high rates of heart tube formation of >90% following casting (supplemental figures 1(e)–(l)). Heart tubes displayed spontaneous and synchronous contractions 3–4 days after casting (movie S1). Confocal images of the heart tube surface revealed dense layers of interconnected cardiomyocytes expressing sarcomeric α -actinin, a marker of z-lines within the myofibrils (figure 2(d)). Higher magnification images confirmed that the cardiomyocytes were differentiated and expressed a dense network of striated myofibrils that were connected between adjacent cells (figure 2(d)). It should be noted that cardiomyocytes did not appear to be aligned.

3.3. Calcium activity and action potential propagation

Electrophysiology of the contractile heart tubes was assessed using calcium imaging during spontaneous and paced contractions. Optical mapping of the engineered heart tube revealed anisotropic conduction along the longitudinal axis, with wavefronts consistently originating at one end and travelling to the other (figure 3(a)). During spontaneous

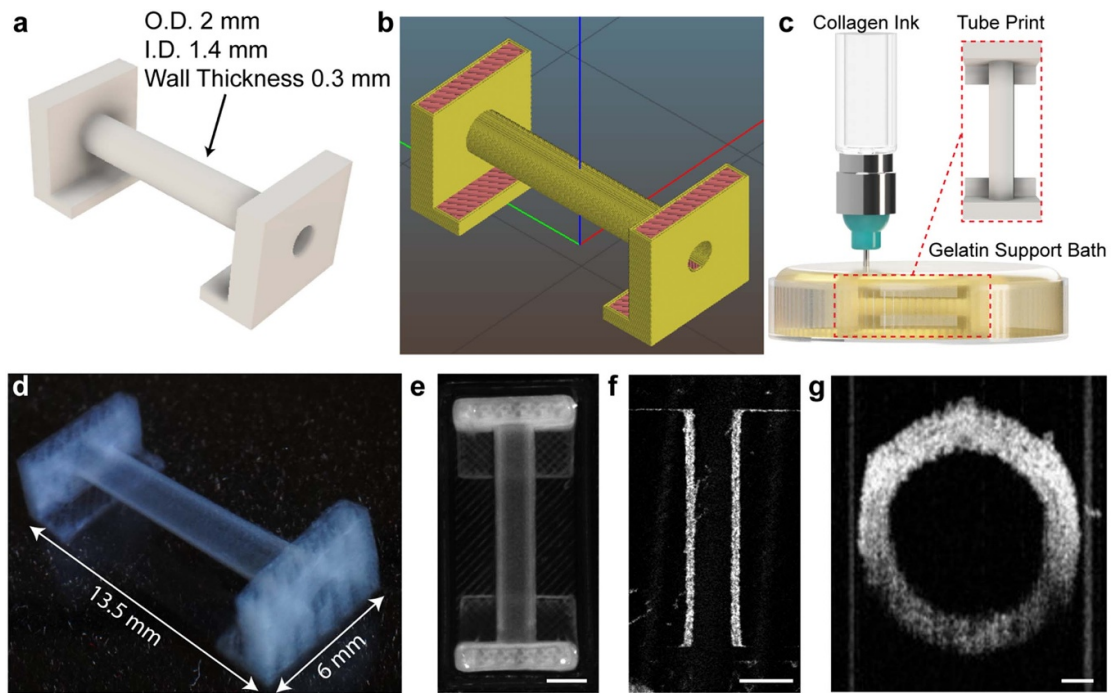


Figure 1. Heart tube printing. (a) A simplified 3D CAD model was first made to represent the linear heart tube. (b) A sliced model was then created to allow layer by layer 3D printing. (c) The collagen tube was printed using freeform reversible embedding of suspended hydrogels (FRESH). Macroscopic images of tube structure in (d) isometric and (e) top down views. (f) A horizontal slice of the 3D OCT image showing the longitudinal axis of the tube and consistent wall thickness. (g) A vertical slice of the 3D OCT image showing the cross-section of the tube and consistent wall thickness. For panels (e) and (f) scale bars are 2 mm, and for panel (g) scale bar is 300 μm .

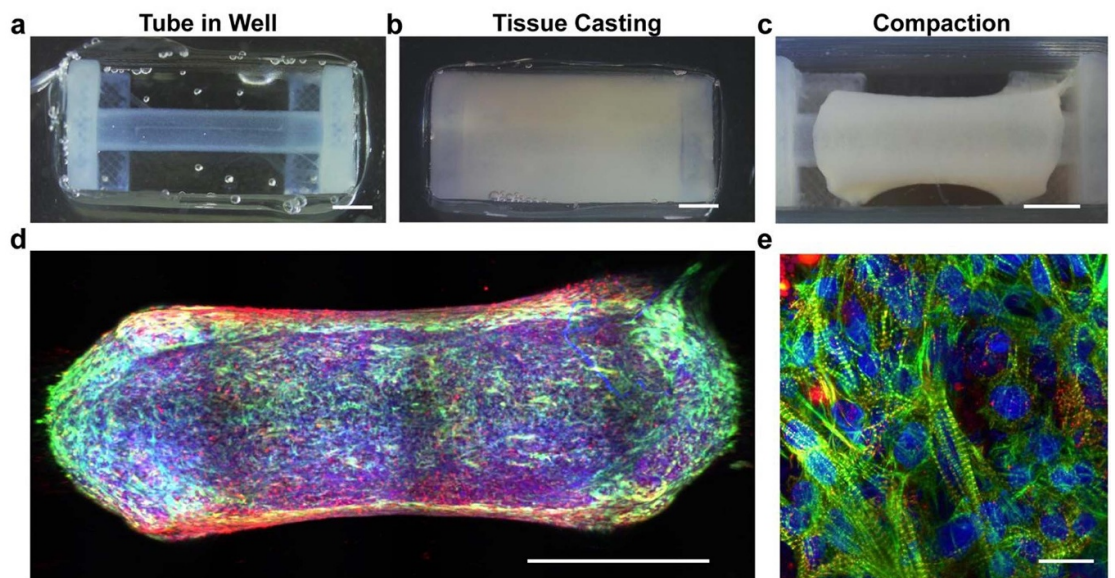
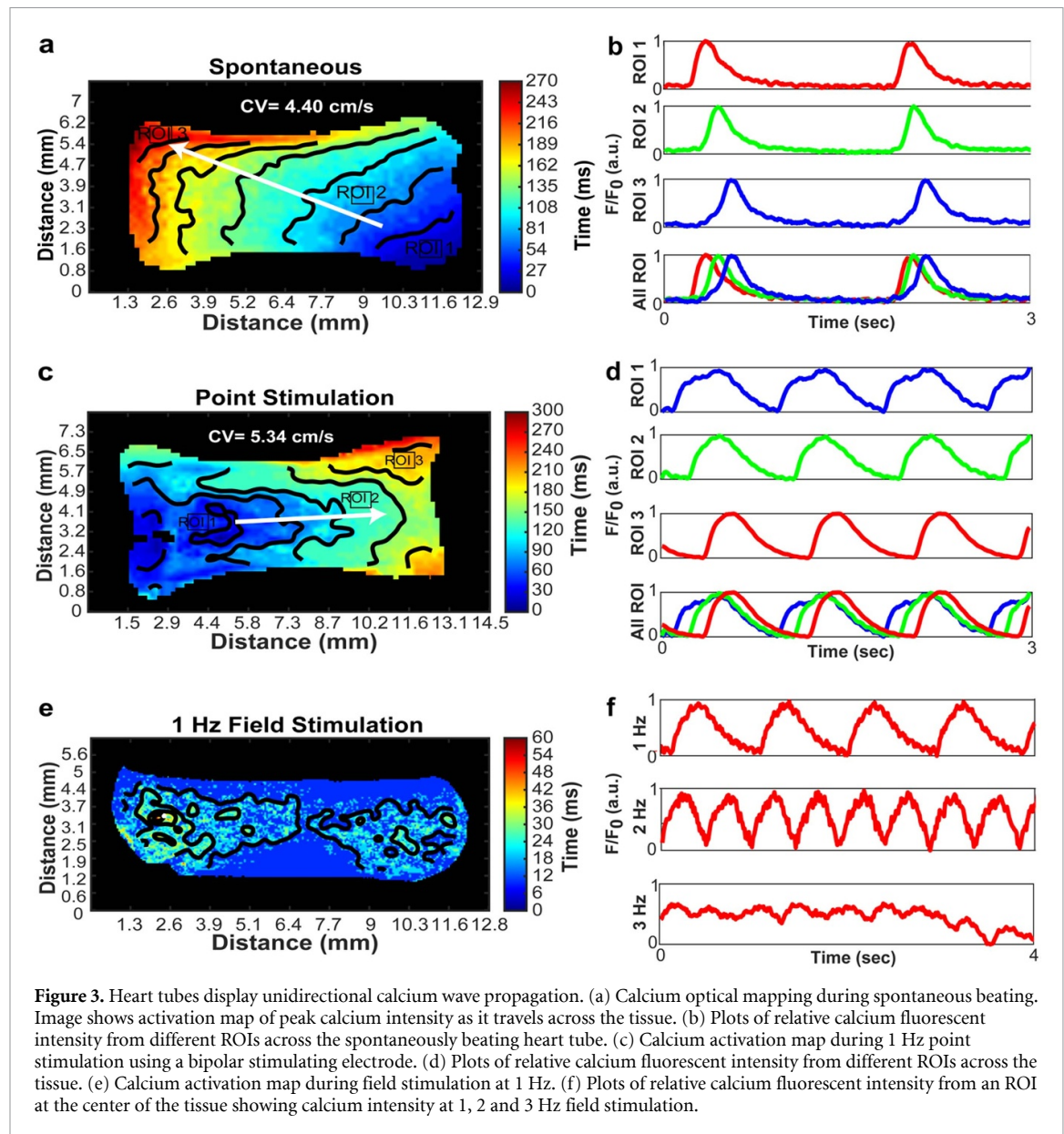


Figure 2. Heart tube formation. (a) The FRESH 3D bioprinted collagen heart tube scaffold is placed inside of a PDMS well to create a chamber for cell seeding. (b) Casting of cardiomyocytes and fibroblasts in a collagen gel around the collagen tube. (c) Cardiac fibroblasts compact the casted collagen gel with cardiomyocytes around the printed collagen tube forming the contractile heart tube. Scale bar is 2 mm. (d) Max intensity projection of heart tube surface showing cardiomyocytes positive for sarcomeric alpha actinin (red), F-actin (green), and DAPI (blue). Scale bar is 2.5 mm. (e) High magnification images of heart tube surface showing densely interconnected and striated cardiomyocytes. Scale bar is 20 μm .

contractions, heart tubes had conduction velocities of $5.44 \pm 1.04 \text{ cm s}^{-1}$ ($n = 7$ heart tubes), which is similar to that observed within the inner curvature of the early embryonic heart tube [22]. Fluorescent

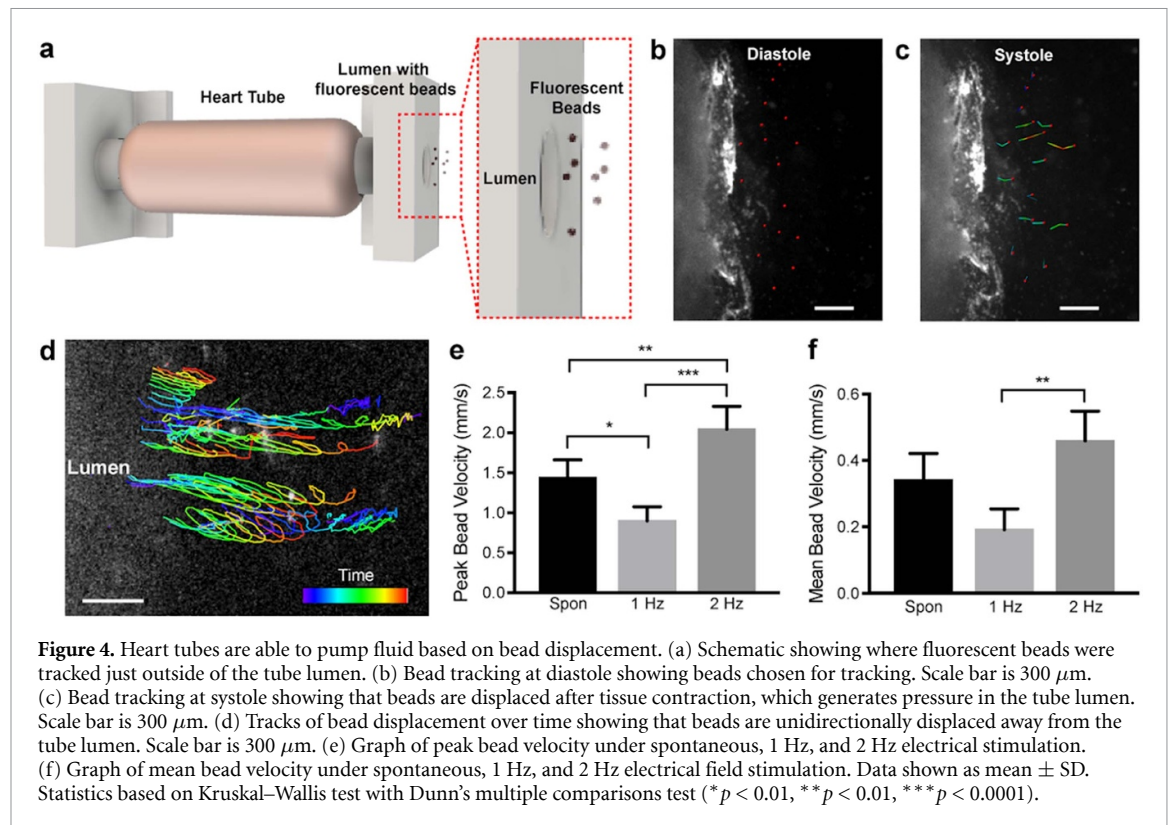
intensity analysis performed at different regions of interest (ROIs) of the heart tube showed similar waveform morphology and expected latency across the tissue (figure 3(b)). Point stimulation at 1 Hz



at one end of the heart tube with a bipolar electrode was used to control the location of initial depolarization and achieve more consistent propagation. In this case we observed a conduction velocity of $4.95 \pm 1.49 \text{ cm s}^{-1}$ (figure 3(c)), which was not statistically different from our average spontaneous conduction velocity measurements. Comparing ROIs across the tissue demonstrated consistent waveform morphology and expected latency across the tissue under point stimulation (figure 3(d)). Heart tubes field stimulated at 1 Hz showed synchronized contraction across the tissue and no calcium wave propagation, as expected (figure 3(e)). Heart tubes were able to be consistently field stimulated at 1 and 2 Hz (movie S2), however, at 3 Hz stimulation most tissues could not be consistently captured and displayed irregular calcium waveforms (figure 3(f)).

3.4. Heart tube contractility

In order to investigate the ability of the engineered heart tubes to pump fluid, $10 \mu\text{m}$ fluorescent beads were injected into the tube lumen and their displacement during contraction was viewed just outside the tube lumen (figure 4(a)). When the tissue was not actively contracting (diastole), beads were identified just outside the tube lumen (figure 4(b)). They were then tracked frame-by-frame during contraction (systole) as the pressure inside the tube lumen increased and beads were displaced (figure 4(c)). When bead displacement was tracked over multiple contractions, unidirectional pumping of the beads away from the tube lumen was observed with the tracks showing individual displacement of single beads (figure 4(d)). Because there are no valves present in the heart tubes, the net displacement was limited as the beds moved



back and forth during the contractile cycle. This suggests that unidirectional calcium wave propagation across the tissue may result in a peristaltic-like wave that displaces beads away from the tube lumen over time; however, further research would be required to confirm this observation. Peak bead velocity was $\sim 1.5\ \text{mm s}^{-1}$, which increased to $\sim 2\ \text{mm s}^{-1}$ following field stimulation at 2 Hz (figure 4(e)). Mean bead velocity was lower at $\sim 0.35\ \text{mm s}^{-1}$ due to the cyclical bead displacement during each contraction, and only a small net displacement was observed. These results clearly show that the heart tube can displace fluid during each contraction, however, valves or other structural features to achieve directional flow are required to achieve higher net displacement.

4. Discussion

The goal of this study was to engineer a simplified model of the heart in the form of a linear heart tube using human ESC-derived cardiomyocytes and assess basic structure, calcium wave propagation and pumping via displacement of fluorescent beads. This tube design was inspired by embryonic development, and the fabrication enabled with the FRESH 3D bioprinting approach [12]. Here, we demonstrated that FRESH can be used to generate linear collagen tubes with high fidelity and that we can use a hydrogel casting approach to create contractile engineered heart tubes. The casting approach was purposely chosen because it enabled very rapid fabrication of the engineered tissue and minimized the amount of time

the ESC-derived human cardiomyocytes were outside of the cell culture incubator.

While we have focused much of our work on the printing of collagen due to our previous work demonstrating high-fidelity printing of cardiac tissue [12], the FRESH technique has been used to print a wide range of bioinks that have the potential to form heart tubes. Our previous work has shown that the FRESH technique supports a wide range of cross-linking mechanisms enabling the printing of different types of bioinks. This can be accomplished by either mixing cross-linking agents within the fluid phase of the support bath, within the bioink itself (depending on the pot life), or via other external mechanisms, such as photocrosslinking. This has allowed for the printing of the broadest range of bioinks within the same platform using pH, temperature, ionic, enzymatic, ‘click’ chemistry and photo crosslinking gelation mechanisms, including published examples using alginate, fibrin, methacrylated hyaluronic acid, methacrylated gelatin, and even concentrated cell bioinks [11, 23–27].

Heart tubes had dense layers of interconnected cardiomyocytes and the spontaneous calcium wave propagation showed anisotropic conduction along the longitudinal axis of the heart tube. However, the cardiomyocytes themselves generally had an isotropic orientation within the tissue, suggesting that the tube shape itself is important for the conduction anisotropy. While the conduction velocity of $\sim 5\text{--}6\ \text{cm s}^{-1}$ is typical for many other cardiac tissues engineered from ESC-derived cardiomyocytes [12, 17, 28, 29],

it is possible that better cell alignment could produce further improvement. Previous research has suggested that mechanical loading [30–33] can guide alignment of cardiomyocytes, and a similar strategy, such as stretching or pressurizing the tube, could be used here to increase cardiomyocyte alignment, which could potentially increase the pumping capability of our engineered heart tubes. Similarly, electrical stimulation [34, 35] can also promote alignment and development of mature calcium handling. These will both be a major focus in our future studies.

Along with mechanical and electrical stimulation, several design features of the printed tube could also be altered to increase the ability of the tube to pump fluid, including decreasing the wall thickness and thus, increasing its ability to be deformed by cardiomyocyte contraction. Similarly, decreasing the tube diameter might also allow for the directional, peristaltic-like contractions seen in the engineered heart tube to further displace fluid out of the tube lumen. Incorporation of features that would ensure unidirectional pumping, such as valves, could also significantly aid pumping by these engineered heart tubes. Previous work has demonstrated the 3D bioprinting of functional valves [12, 36], and incorporating these will also be the focus of future work.

In comparison to embryonic development, the maximum pumping velocity we observed in our engineered heart tube is much lower than that observed in the embryonic linear heart tube, which ranges from 5 to 25 cm s⁻¹ based on the developmental stage of the chick embryonic heart [37]. However, we did achieve increased flow rates when comparing our work to other skeletal and heart muscle engineered tissue pumps, or so called ‘pump bots’. For instance, Park *et al* developed a hybrid micropump consisting of a dome-shaped membrane with attached cardiomyocytes to generate unidirectional displacement of beads at 3.78 μm s⁻¹, which is less than the average pumping velocity observed in our engineered heart tube [38]. Similarly, Li *et al* created an impedance pump bot consisting of an engineered skeletal muscle ring wrapped around PDMS tubing and was able to achieve a maximum average flow rate of 39.9 μm s⁻¹, which is approximately an order of magnitude less than the average flow we were able to achieve with our engineered heart tube [39]. This could be due to the relative increase in size of our engineered heart muscle tissue compared to their much smaller skeletal muscle tissue ring; however, future work would need to be performed to validate this observation.

Finally, our design is a simplification of the embryonic linear heart tube shape and size. As noted, our engineered heart tube is larger than the embryonic heart tube (~1.4 mm versus ~300 μm inner diameter). However, we wanted to test our design concept at this larger scale before printing the much smaller embryonic heart tube. We believe that

we can FRESH 3D print smaller heart tubes but will need to improve our print resolution using smaller collagen filaments to decrease the wall thickness.

Despite these limitations, being able to engineer the heart tube is a novel biofabrication approach and we are not aware of other research that is able to generate a contractile, beating heart tube composed of human cardiomyocytes using a bioprinting approach. Several studies have demonstrated the utility of bioprinting heart muscle sheets to repair the heart following acute MI [40]; however, very few studies have been able to bioprint more complex 3D structures that are capable of performing functions associated with human heart, such as pumping fluid [26]. Recent reports printing heart tube structures with photocurable resins did not incorporate cardiomyocytes, and thus, were unable to assess heart tube contractile function, like calcium wave propagation and pumping capability [41]. While other bioprinting methods have been utilized, including assembly of cardiac spheroids on needle arrays into a tube-like shape, the contractility of these tubes was not thoroughly assessed [42]. Most other methods have manually wrapped engineered heart tissues into a tube-like structures to create a contractile heart tubes [43, 44]. The advantage of our FRESH bioprinting approach over these examples is the ability to easily tailor the structure of the collagen tube. Our future work will focus on investigating more advanced heart tube structure and function, with the goal to increase contractility and begin to mimic aspects of cardiac development such as heart tube bending and looping.

5. Conclusion

In conclusion, we have engineered a contractile human heart tube inspired by early embryonic development. We have demonstrated that the heart tubes have dense layers of cardiomyocytes on their surface, display unidirectional calcium wave propagation, and are able to be electrically paced up to 2 Hz. Heart tubes were also able to displace fluorescent beads via generation of increased pressure within the tube lumen with each contraction.

Data availability statement

The data that support the findings of this study are available upon reasonable request from the authors.

Acknowledgments

This work was supported by the Additional Ventures Cures Collaborative (to A F), the Office of Naval Research (Grant Number N00014-17-1-2566 to A F), the Food & Drug Administration (Grant Number R01FD006582 to A F), the Dowd Fellowship (to J B) and the Carnegie Mellon Presidential Fellowship (to J B).

Author contributions

J B and A F designed the research; J B, J T, M S, B C, D S, A L, T H performed the research; J B, J T, D S analyzed data; and J B, A F wrote the paper.

Conflict of interest

A L, T H, and A F all have an equity stake in FluidForm Inc. which is a startup company commercializing FRESH 3D printing. FRESH 3D printing is the subject of patent protection including U.S. Patent 10150258 and others.

ORCID iDs

Jacqueline Bliley  <https://orcid.org/0000-0002-6605-9916>

Joshua Tashman  <https://orcid.org/0000-0001-8193-0039>

Maria Stang  <https://orcid.org/0000-0001-8700-6904>

Brian Coffin  <https://orcid.org/0000-0001-7256-8525>

Daniel Shiwarski  <https://orcid.org/0000-0001-6978-303X>

Andrew Lee  <https://orcid.org/0000-0001-5174-4999>

Thomas Hinton  <https://orcid.org/0000-0001-8784-3710>

Adam Feinberg  <https://orcid.org/0000-0003-3338-5456>

References

- [1] Savarese G and Lund L H 2017 Global public health burden of heart failure *Card. Fail. Rev.* **03** 7
- [2] Virani S S et al 2020 Heart disease and stroke statistics—2020 update: a report from the American Heart Association *Circulation* **141** e139–e596
- [3] Kilic A and Ailawadi G 2012 Left ventricular assist devices in heart failure *Expert Rev. Cardiovasc. Ther.* **10** 649–56
- [4] Deng M 2002 Cardiac transplantation *Heart* **87** 177–84
- [5] Tzahor E and Poss K D 2017 Cardiac regeneration strategies: staying young at heart *Science* **356** 1035–9
- [6] Batalov I and Feinberg A W 2015 Differentiation of cardiomyocytes from human pluripotent stem cells using monolayer culture *Biomark. Insights* **10** 71–76
- [7] Laflamme M A et al 2007 Cardiomyocytes derived from human embryonic stem cells in pro-survival factors enhance function of infarcted rat hearts *Nat. Biotechnol.* **25** 1015–24
- [8] Chong J J H et al 2014 Human embryonic-stem-cell-derived cardiomyocytes regenerate non-human primate hearts *Nature* **510** 273–7
- [9] Vunjak-Novakovic G, Tandon N, Godier A, Maidhof R, Marsano A, Martens T P and Radisic M 2010 Challenges in cardiac tissue engineering *Tissue Eng. B* **16** 169–87
- [10] Mandrycky C J et al 2020 Engineering heart morphogenesis *Trends Biotechnol.* **38** 835–45
- [11] Hinton T J, Jallerat Q, Palchesko R N, Park J H, Grodzicki M S, Shue H J, Ramadan M H, Hudson A R and Feinberg A W 2015 Three-dimensional printing of complex biological structures by freeform reversible embedding of suspended hydrogels *Sci. Adv.* **1** e1500758
- [12] Lee A, Hudson A R, Shiwarski D J, Tashman J W, Hinton T J, Yerneni S, Bliley J M, Campbell P G and Feinberg A W 2019 3D bioprinting of collagen to rebuild components of the human heart *Science* **365** 482–7
- [13] Lian X, Zhang J, Azarin S M, Zhu K, Hazeltine L B, Bao X, Hsiao C, Kamp T J and Palecek S P 2013 Directed cardiomyocyte differentiation from human pluripotent stem cells by modulating Wnt/ β -catenin signaling under fully defined conditions *Nat. Protocols* **8** 162–75
- [14] Burridge P W et al 2014 Chemically defined generation of human cardiomyocytes *Nat. Methods* **11** 855–60
- [15] Tohyama S et al 2013 Distinct metabolic flow enables large-scale purification of mouse and human pluripotent stem cell-derived cardiomyocytes *Cell Stem Cell* **12** 127–37
- [16] Tashman J W, Shiwarski D J and Feinberg A W 2021 A high performance open-source syringe extruder optimized for extrusion and retraction during FRESH 3D bioprinting *HardwareX* **9** e00170
- [17] Bliley J M et al 2021 Dynamic loading of human engineered heart tissue enhances contractile function and drives desmosome-linked disease phenotype *Sci. Trans. Med.* **13** eabd1817
- [18] Huebsch N et al 2016 Miniaturized iPSC-cell-derived cardiac muscles for physiologically relevant drug response analyses *Sci. Rep.* **6** 24726
- [19] Radisic M, Park H, Martens T P, Salazar-Lazaro J E, Geng W, Wang Y, Langer R, Freed L E and Vunjak-Novakovic G 2008 Pre-treatment of synthetic elastomeric scaffolds by cardiac fibroblasts improves engineered heart tissue *J. Biomed. Mater. Res. A* **86A** 713–24
- [20] Thavandiran N et al 2013 Design and formulation of functional pluripotent stem cell-derived cardiac microtissues *Proc. Natl Acad. Sci. USA* **110** E4698–707
- [21] Zhao Y et al 2019 A platform for generation of chamber-specific cardiac tissues and disease modeling *Cell* **176** 913–27.e18
- [22] Gu S, Wang Y T, Ma P, Werdich A A, Rollins A M and Jenkins M W 2015 Mapping conduction velocity of early embryonic hearts with a robust fitting algorithm *Biomed. Opt. Express* **6** 2138–57
- [23] Shiwarski D J, Hudson A R, Tashman J W and Feinberg A W 2021 Emergence of FRESH 3D printing as a platform for advanced tissue biofabrication *APL Bioeng.* **5** 010904
- [24] Mirdamadi E, Tashman J W, Shiwarski D J, Palchesko R N and Feinberg A W 2020 FRESH 3D bioprinting a full-size model of the human heart *ACS Biomater. Sci. Eng.* **6** 6453–9
- [25] Pusch K, Hinton T J and Feinberg A W 2018 Large volume syringe pump extruder for desktop 3D printers *HardwareX* **3** 49–61
- [26] Kupfer M E et al 2020 *In situ* expansion, differentiation and electromechanical coupling of human cardiac muscle in a 3D bioprinted, chambered organoid *Circ. Res.* **127** 207–24
- [27] Hull S M, Lindsay C D, Brunel L G, Shiwarski D J, Tashman J W, Roth J G, Myung D, Feinberg A W and Heilshorn S C 2021 3D Bioprinting using universal orthogonal network (UNION) bioinks *Adv. Funct. Mater.* **31** 2007983
- [28] Song H et al 2010 Interrogating functional integration between injected pluripotent stem cell-derived cells and surrogate cardiac tissue *Proc. Natl Acad. Sci. USA* **107** 3329–34
- [29] Spencer T M, Blumenstein R F, Pryse K M, Lee S L, Glaubke D A, Carlson B E, Elson E L and Genin G M 2017 Fibroblasts slow conduction velocity in a reconstituted tissue model of fibrotic cardiomyopathy *ACS Biomater. Sci. Eng.* **3** 3022–8
- [30] Leonard A, Bertero A, Powers J D, Beussman K M, Bhandari S, Regnier M, Murry C E and Sniadecki N J 2018 Afterload promotes maturation of human induced pluripotent stem cell derived cardiomyocytes in engineered heart tissues *J. Mol. Cell. Cardiol.* **118** 147–58

- [31] Hirt M N *et al* 2012 Increased afterload induces pathological cardiac hypertrophy: a new *in vitro* model *Basic Res. Cardiol.* **107** 307
- [32] Zimmermann W H, Melnychenko I and Eschenhagen T 2004 Engineered heart tissue for regeneration of diseased hearts *Biomaterials* **25** 1639–47
- [33] Boudou T, Legant W R, Mu A, Borochin M A, Thavandiran N, Radisic M, Zandstra P W, Epstein J A, Margulies K B and Chen C S 2012 A microfabricated platform to measure and manipulate the mechanics of engineered cardiac microtissues *Tissue Eng. A* **18** 910–9
- [34] Radisic M, Park H, Shing H, Consi T, Schoen F J, Langer R, Freed L E and Vunjak-Novakovic G 2004 Functional assembly of engineered myocardium by electrical stimulation of cardiac myocytes cultured on scaffolds *Proc. Natl Acad. Sci. USA* **101** 18129–34
- [35] Ronaldson-Bouchard K, Ma S P, Yeager K, Chen T, Song L J, Sirabella D, Morikawa K, Teles D, Yazawa M and Vunjak-Novakovic G 2018 Advanced maturation of human cardiac tissue grown from pluripotent stem cells *Nature* **556** 239–43
- [36] Grigoryan B *et al* 2019 Multivascular networks and functional intravascular topologies within biocompatible hydrogels *Science* **364** 458–64
- [37] Butcher J T, McQuinn T C, Sedmera D, Turner D and Markwald R R 2007 Transitions in early embryonic atrioventricular valvular function correspond with changes in cushion biomechanics that are predictable by tissue composition *Circ. Res.* **100** 1503–11
- [38] Park J, Kim I C, Baek J, Cha M, Kim J, Park S, Lee J and Kim B 2007 Micro pumping with cardiomyocyte-polymer hybrid *Lab Chip* **7** 1367–70
- [39] Li Z, Seo Y, Aydin O, Elhebeary M, Kamm R D, Kong H and Taher Saif M A 2019 Biohybrid valveless pump-bot powered by engineered skeletal muscle *Proc. Natl Acad. Sci. USA* **116** 1543–8
- [40] Kim K S *et al* 2021 Transplantation of 3D bio-printed cardiac mesh improves cardiac function and vessel formation via ANGPT1/Tie2 pathway in rats with acute myocardial infarction *Biofabrication* **13** 045014
- [41] Cetnar A D *et al* 2020 Patient-specific 3D bioprinted models of developing human heart *Adv. Healthcare Mater.* **2001169** 1–15
- [42] Arai K, Murata D, Verissimo A R, Mukae Y, Itoh M, Nakamura A, Morita S and Nakayama K 2018 Fabrication of scaffold-free tubular cardiac constructs using a Bio-3D printer *PLoS One* **13** e0209162
- [43] Park J *et al* 2020 Modular design of a tissue engineered pulsatile conduit using human induced pluripotent stem cell-derived cardiomyocytes *Acta Biomater* **102** 220–30
- [44] Biermann D *et al* 2016 Towards a tissue-engineered contractile fontan-conduit: the fate of cardiac myocytes in the subpulmonary circulation *PLoS One* **11** e0166963